

D.J. Warner

CERN, Geneva, Switzerland

Introduction

The basic parameters of the machine and the preliminary proposals for the experimental programme of the CERN 3 MeV linac were reported at a previous linac conference.(1) In this paper, the intention is to show how the project has developed since 1968 and to bring together some experimental results which have not yet been published or only published in part. It can be stated immediately that the original scheme of experiments, that is a gradual process of calibration and checking against computed results eventually leading to a detailed description of the linac proton dynamics under extreme space-charge conditions, has not been followed. There were several reasons for this, the most important being our early observations that neutralization of the proton beam at 500 keV played a predominant role in the dynamics before the linac and, further, that comprehensive emittance and energy spread measurements over a large range of operating conditions require either a prohibitive amount of manual data collection or a sophisticated automatic data collection scheme.

Thus, in addition to the operation and measurements at 3 MeV with beam currents  $\sim 200$  mA, a significant part of our experimental work has concerned the 500 keV beam, e.g. neutralization (2), effect of secondary electrons on emittance measurements (3), and the development of a broad band coaxial probe to make real-time measurements of the proton bunch form.(4)

For general proton linac development, the framework and facilities of the 3 MeV linac have been extensively employed: (a) as a specific example for development of computer programs for cavity calculations (5), buncher calculations by multiparticle programs and linac dynamics with space charge (6); (b) as a test-bed for systems and components to be installed on the 50 MeV linac, especially source, high-voltage level compensation (7) and RF systems; (c) as a realistic model for trying out a different approach to the mechanical problems posed by a copper-clad structure with single support stem for the drift tubes.

Parameters of the 3 MeV Linac

In this section, the principal parameters of the 3 MeV linac are given. The standard 'form' is used in Table I for ease of comparison with other linacs and additional information given to complement this. It should be emphasized again that the dimensions and shapes of cavity and drift tubes are based directly on the first 18 cells of the 0.5 MeV to 10 MeV section of the CERN 50 MeV linac. In fact, the only differences in the shapes and dimensions of the drift tubes of the 3 MeV accelerator are that the apertures and 'hole-corner' radii vary more smoothly along the system. The cell and drift-tube lengths increase linearly with the cell number to give a nearly constant accelerating rate along the cavity. As  $g/L$  remains constant along the tank, the drift-

tube diameter and profile are changed to maintain resonance as the cell length increases. The drift-tube outer diameters fall monotonically (but not linearly) with cell number, while the outer part of the drift-tube section is a semi-ellipse on an axis  $\sim 13$  mm from the drift-tube axis. This varying geometry is advantageous in having low RF dissipation, but it creates difficulties when fitting in quadrupoles, compared with cylindrical drift tubes. Each drift tube is supported by a single vertical stem (28 mm outer diameter) from a rigid girder arranged so that the set of 17 drift tubes can be put in the tank together after mounting and alignment. Some mechanical engineering and manufacturing details are given in a previous paper.(1)

Some Calibrations Made at the Assembly Stage

In this section some of the important calibrations which are relevant to the subsequent performance of the machine are described briefly.

Pulsed Quadrupoles

The drift-tube quadrupole design follows that described in Regenstreif (8) except for the first three lenses which have a more efficient pole form. The yoke outside diameter is constant at 60 mm, the aperture diameter varies in steps (20 mm, 24 mm, and 30 mm), while the length varies continuously to fill each drift tube with a roughly constant filling factor (iron),  $\sim 0.48 (L_q/L_n)$ . Each quadrupole was calibrated with a Hall probe measuring apparatus before mounting in its drift tube. The following measurements were made. (a) The excitation curve gradient ( $B'$ ) versus current ( $I$ ). (b) The magnetic length via a point-by-point field plot. (c) The position of magnetic centre relative to the mechanical centre defined by the yoke (only two quadrupoles with  $> 0.05$  mm error). (d) The position of the neutral planes relative to a key-way in the yoke. Before mounting the drift tubes in the cavity a check on the quadrupole excitation curve was made with a long integrating search coil up to twice the normal +--- excitation current. A potentiometric comparison method was used and results could be expressed in the form:

$$B'/I = \alpha_0 + \alpha_1 I^2 + \alpha_2 I^4 . \quad (1)$$

This equation was especially useful for interpolation in the saturation region.

Drift-Tube Alignment

For the length of the 3 MeV linac a micro-alignment telescope is easy to use precisely. The drift tubes could be aligned relative to each other outside the resonator when the support girder was raised. Attached to the girder are the alignment adjustment mechanisms, which provide a vertical adjustment directly and the horizontal and axial movements by rotation of the support stem in a spherical bearing with the arm of rotation ( $\sim 500$  mm) introducing negligible angular errors. For the initial

alignment of the system, the two end half drift tubes were used to define an axis for the cavity, the low-energy drift space (Fig. 1) and the pre-injector. The first and last complete drift tubes (Nos. 2 and 18) were then aligned to this axis with the girder bolted down. With the girder raised the other drift tubes were accessible for adjustment of gaps followed by alignment transversely relative to tubes Nos. 2 and 18. As the maximum sighting distance was only 3 m, the radial tolerance of 0.10 mm was not difficult to obtain.

We found that the adjustment mechanisms were a big improvement on the devices used with two stem drift tubes on the 50 MeV linac. In particular, the movement was continuous and predictable against spring loading, with the drift tube returning quickly to its aligned position when accidentally displaced.

#### Low-Power RF Measurements

The usual measurements were made on the assembled cavity, viz. input loop match (and Q), axial field measurements by perturbation, ball tuner calibration and monitoring loop calibration.

There are two input feed loops, one for cavity excitation and the other, not yet operational, for beam-loading compensation. Each loop is matched when the cavity is on tune and the other loop short-circuited. The Q, measured via the variation of feed loop match with frequency is 48,000, 80% of the estimated perfect copper value.

Measurements of axial field distribution were made by perturbation with a 5 mm bead drawn along the cavity axis. The frequency perturbation ( $\sim 550$  Hz peak) was measured and plotted on a chart recorder. To compare the results with the theoretical requirements, the peak field in each gap was normalized by the computed axial field distribution in the cell to give the corresponding mean field. The mean fields fell within  $\pm 1.5\%$  of the required field when the ball tuners were all at the same radial position so no further correction was done. These five tuners, equally spread along the cavity, have a total measured range of +175 kHz and -600 kHz about 202.56 MHz. They could be used to tilt the electric field so that it increased or decreased by 3% over the length of the cavity relative to the design field, but this was not found useful in practice. The monitoring loops were set for a nominal coupling -55 dB relative to the main input loop power; during beam measurements it was preferable to calibrate the indicated RF level with the acceleration threshold.

#### Initial Operation with a 3 MeV Beam

The principal stages in the improvement of the output beam are given briefly here with a detailed account of the RF problems left to the next section.

Generally the major improvements in current or beam quality were associated with the installation of apparatus or the diagnosis of a particular fault. Thus, for the initial operation in November 1969, there was no buncher, no bending magnet and no experimental area focusing. The 3 MeV beam was

detected after passing through aluminium foils in front of the measuring transformer and was typically 30 mA (50 mA) for  $N = 2$  ( $N = 1$ ) focusing. After installation of the buncher and an intermediate electrode in the accelerating column and then realignment of the pre-injector, 110 mA (150 mA) was obtained with  $N = 2$  ( $N = 1$ ) focusing. The next major improvement came after installation of the  $18^\circ$  bending magnet, the 3 MeV triplet (T3), an improved ion source, and some adjustments on the quadrupole pulsers to allow higher current operation. Since then  $> 130$  mA ( $> 200$  mA) of analysed 3 MeV protons have been regularly obtained with  $N = 2$  ( $N = 1$ ) focusing.

#### Some RF Problems

##### First Trials with the Main Cavity

Experience with the same RF structure on the 50 MeV linac led us to expect some difficulties with multipactor during the initial RF trials, although the pressure in the 3 MeV cavity was  $\sim 1.5 \times 10^{-9}$  Torr. In fact, after about 6 hours running, up to 200 kW was being accepted by the cavity with about 25% missed pulses, but only when neither the ionization gauge nor the triode ion pump were on. This condition would not entirely prevent operation because nearly half the pumping speed is provided by a turbomolecular pump. Although there were measurable improvements after leaking hydrogen or nitrogen into the cavity to provide some scouring action, the problem persisted until the timing between the drive and main modulators was adjusted (presumably to obtain a faster rate of rise of RF power) and then power was reliably accepted with both gauge and ion pump working. After several weeks without RF power in the cavity it sometimes requires about one hour's conditioning to reach operating level reliably.

On the 3 MeV, as on other linacs, sparking occurs predominantly between the first few drift tubes leaving white marks which are not particularly associated with maximum electric field regions. However, in our case, persistent sparking was not required to condition the surface and raise the breakdown threshold. A gradual increase in level, always keeping about 2% below the breakdown threshold, was much more effective. At high field levels characteristic points of light could be seen on the drift-tube faces and X-rays became a personnel hazard. Measurements have been made with a proton beam up to an equivalent synchronous phase of  $55^\circ$ , corresponding to a peak surface electric field of  $20 \text{ MV m}^{-1}$  on the first drift tube.

##### Buncher Problems

The buncher is a simple re-entrant cavity with essentially the same geometry (internally) as the original buncher of the 50 MeV linac. Two particular features of the 3 MeV buncher are: (a) a biased plate is used for the suppression of multipactoring; this plate effectively forms one end of the cavity; (b) operation is without grids and the beam aperture is 18 mm diameter.

Even with bias applied, several hours operation were required initially before RF power was accepted reliably. The improvement one sees during months of operation is that the bias can be reduced to zero and

that lower RF levels can be obtained stably. Another difficulty, which was confused at first with the conditioning process, was a pulse-to-pulse variation in input match (as indicated on the input power reflectometer). This was eventually traced to mechanical oscillations of the bias plate which was supported at three points near its edge. After wedging the plate near its centre, a distinct improvement in beam stability was observed; this stability is fundamental for obtaining high current performance at low repetition rate (1 pps).

#### Beam Loading

The beam-loading compensation system has not yet been used on the 3 MeV accelerator, so that when large currents are accelerated the RF envelope has a characteristic droop during the beam pulse. This droop is typically  $1\%/\mu\text{sec}$  for a 200 mA accelerated proton beam and it leads to a rounded top on the current pulse when near optimum RF level. During beam measurements all readings are taken at a fixed time in the pulse to avoid errors due to this time variation of RF level.

For the buncher, the theory dictates that beam loading is a second-order effect arising from the variation of transit time factor with proton energy averaged across the gap. Thus marked loading, as inferred from the buncher RF envelope, is an indication of slower ions or electrons taking energy from the gap. On the 3 MeV accelerator this loading effect is typically less than 5% (and constant over most of the beam pulse). However, it has been up to 12% and lower than 1% without any apparent correlation with beam current or pressure.

#### Measurements with the 500 keV Beam

Much of the experimental work on the 3 MeV project has been with the 500 keV beam and the studies of self-neutralization (2), the effect of secondary electrons on emittance measurements (3), and the development of a broad band probe for studying proton bunches (4) have been published. The results of the more controversial topics can be summarized as follows.

- a) With high current beams at 500 keV, self-neutralization of the beam occurred both in regions of high gas pressure and in places where one has to postulate electron migration from another area or copious secondary electrons arising from lost protons.
- b) The neutralization persists in the presence of magnetic fields but can be suppressed locally with positively biased electrodes.
- c) When the space charge contribution to the beam motion is significant compared to the emittance effect, secondary electrons from the first defining slits can falsify the results of an emittance measurement. The principal effect is to rotate the emittance without changing its magnitude, which during our measurements was  $\epsilon_{\text{rms}} \approx 1.8\pi \times 10^{-6}$  rad m (normalized) for 240 mA at 500 keV.
- d) Biasing the defining slits (positively) can suppress any neutralizing electrons that are already present in the beam. For optimum beam transfer into the 3 MeV some self-neutralization is apparently

necessary so the prospects for precise emittance measurements at the input are not good.

In any future accelerator we would aim to provide more quadrupole focusing per unit axial length in a longer low-energy drift space in order to match the beam to the linac with less dependence on space charge (or neutralization). Any emittance slits would be positively biased to suppress secondary electrons.

#### Some Measurements Made During High Current Operation

In this section a brief summary is given of measurements on the 3 MeV beam done to compare operation with  $N = 2$  and  $N = 1$  focusing and also to compare the beam quality obtained at 3 MeV with that specified at 50 MeV.

#### Setting Up the 3 MeV Beam

The method of setting up the beam was an empirical optimization for maximum beam through the last measuring transformer (BM7) in the experimental area (Fig. 1). This is not an ideal way of getting a matched beam but there are some practical points in its favour. (a) The beam transport after the accelerator does define a beam of reasonable quality. (b) There are only two triplets and one buncher to optimize in the low-energy drift space (LEDS). (c) In previous papers we have shown that when space-charge neutralization is likely, measurements and calculations of beams in the LEDS are liable to large errors. (d) Some final empirical optimization is often necessary even when sophisticated measuring apparatus is available.

In Table II the currents achieved by the 3 MeV are given for +- ( $N = 1$ ) and +--+ ( $N = 2$ ) focusing. The detailed measurements of emittance and energy spread given below are for currents  $< 80\%$  of these maxima. (To change from  $N = 2$  to  $N = 1$  configuration the connections to eight quadrupoles have to be reversed.) Factors which limit the maximum current at 3 MeV are the source condition and the LEDS transport for both modes of operation and the transport into the 'experimental area' (HEDS) for  $N = 1$  only. Thus best results correspond to exceptionally large source currents ( $\sim 700$  mA) which give  $\sim 400$  mA into the accelerator proper. But for these high currents a quadrupole triplet (T2) is insufficient to match into the linac a beam with general orientation in transverse phase space. In practice, the first quadrupoles in the tank are also used in the matching process and the setting of triplet T1 is critical. For  $N = 1$  focusing some quadrupoles are run into saturation with the power supplies at their limits; where the quadrupoles operate within their range of calibration the gradients fall on a tolerably smooth law,  $\beta^{-n}$ . With high beam currents the transport through the  $18^\circ$  bend is critical and to match into the emittance-measuring apparatus, the last two drift-tube quadrupoles, the bending magnet and two elements of triplet T3 are used. But this limited acceptance of the HEDS does ensure a reasonable beam quality at the measuring apertures BA4 and BA5.

## A Simple Comparison of N = 1 and N = 2 Operation

An experiment which compares N = 1 with N = 2 operation is the measurement of currents as a function of RF level before and after momentum analysis with apertures BA4 and BA5 set to 20 mm × 20 mm (Fig. 2). The optimum synchronous phases are ~ 39° and 29° for N = 1 and N = 2, respectively. The currents at BM7 are much closer to the currents measured at BM5 for N = 2. In comparison, the N = 1 system retains more low-energy particles below and above accelerating threshold and accommodates a beam of poor quality at high RF levels.

### Emittance Measurements

From the emittance measurements one can study the dependence of the transverse beam quality on the various modes of operation. In Table III there are some results for the vertical plane (z, z'). The corresponding values for the horizontal plane (y, y') are generally larger as the dispersion of the magnet and any field or energy variations will contribute to the measured emittances. The two-slit method was used (3) with separation of slit assemblies of 0.53 m. Slits 1 mm wide were used in both positions to obtain good resolution via the emittance analysis program, EMITNC. Each current recorded corresponds to an unnormalized phase-space area ~ 1.9 mm mrad and up to 300 elemental currents  $\{(\Delta I_i)\}$  are required to represent a complete phase plane. We confirmed the hypothesis that, compared to the 500 keV case, the smaller space charge parameter and secondary emission coefficient at 3 MeV would make it unnecessary to bias the front slits to obtain consistent results. In Table III the emittance is given in three forms. (a) By  $\epsilon_0$ , the normalized emittance which contains 63% of the current and which comes from the hypothetical relation between current and emittance:

$$I = I_{\text{tot}} [1 - \exp(-\epsilon/\epsilon_0)] \quad (2)$$

(b) By an r.m.s. emittance

$$\epsilon_{\text{rms}}/(\beta\gamma) = 4[\tilde{z}^2 \tilde{z}'^2 - (\tilde{z}\tilde{z}')^2]^{1/2} \quad (3)$$

with

$$\tilde{z} = \left[ \left( \sum_{i=1}^N z_i^2 \Delta I_i \right) / I_{\text{tot}} \right]^{1/2}$$

and with N the number of current elements and  $I_{\text{tot}}$  the total current. Similar relations are used for  $\tilde{z}'$  and  $(\tilde{z}\tilde{z}')^{1/2}$ . (c) By  $\epsilon_{100}$ , the normalized emittance which contains 100 mA.

If the current is distributed in the phase plane like a two-dimensional Gaussian then Eq. (2) applies,  $\epsilon_{\text{rms}}$  is  $2\epsilon_0$  and current within  $\epsilon_{\text{rms}}$  would be 0.86  $I_{\text{tot}}$ . For all the results analysed  $\epsilon_{\text{rms}}$  has contained between 0.87  $I_{\text{tot}}$  and 0.91  $I_{\text{tot}}$ . Note that in program EMITNC the current is calculated within equidensity contours so that results will be optimistic if the emittance is very distorted. The emittances measured on the 3 MeV were sometimes slightly distorted towards the periphery, but the denser regions were more nearly elliptical (Fig. 3).

## Energy Spectra at 3 MeV

Energy spread measurements were made to compare the operation at N = 1 and N = 2 with and without pre-buncher. For these the object slit (BA3) was set to ~ 0.2 mm and the beam sample was focused in the image plane (BA5) by two elements of T3. This arrangement gave  $\Delta E/E = 0.8\%/mm$  and normally currents via a 0.2 mm slit (BA5) were recorded every 0.5 mm. In Fig. 4 we show a set of results for N = 1 operation with buncher, over the range of RF levels from threshold to breakdown. There is little of the characteristic structure one obtains with low current paraxial beams. Up to the normal optimum level (6.50 V nominal field) the full width at half-maximum measure of  $\Delta E/E$  is < 3% (i.e. < ±45 keV), but  $\Delta E/E$  rapidly deteriorates above this level. This behaviour is characteristic of all the high current measurements for N = 1 and N = 2, though without pre-bunching there is more fine structure in the spectra.

### Discussion of Results

Assuming that the results can be extrapolated to 50 MeV without loss in quality, one can make the comparison with the beam specified for injection into the CERN booster synchrotron, i.e. 100 mA in  $30\pi \times 10^{-6}$  rad m ( $10\pi \times 10^{-6}$  rad m normalized by  $\beta\gamma$ ) and within ±150 keV after complete debunching. With the 3 MeV accelerator (N = 1 focusing) one obtains either 100 mA within  $1.9\pi \times 10^{-6}$  (norm.  $\beta\gamma$ ) rad m or 162 mA within  $10\pi \times 10^{-6}$  (norm.  $\beta\gamma$ ) rad m. If the non-space charge adiabatic relation holds,  $\Delta E$  will vary as  $\beta^{3/4}$  and  $\Delta E_{50 \text{ MeV}} \approx 2.8 \Delta E_{3 \text{ MeV}}$ , i.e. ±150 keV at 50 MeV corresponds to ±54 keV at 3 MeV. Within this energy interval there is (according to the results of Fig. 4) 100 mA.

A result which is as significant as the above is that, at 3 MeV, N = 1 operation gives 100 mA within a much smaller emittance and within a much smaller energy spread than does N = 2 operation.

### Blow-up Between 500 keV and 3 MeV

Due to lack of direct input/output comparisons only informed guesses can be offered for emittance blow-up and phase-space dilution. Assume first that the input beam fills the acceptance [as computed by Weiss and Bru (9)] and using the  $\epsilon_{\text{rms}}$  of results 1 and 2 in Table III one obtains increases in emittance by × 1.8 and × 1.3, respectively. For phase-space dilution, compare the central densities of results 1 and 2 with the measured density at 500 keV (288 mA/π mm mrad) and assume transmission loss of 0.55 longitudinally. This gives dilutions of 2.8 and 2.0, respectively. Without the correction for trapping, one obtains the direct ratios between input and output central densities, representing the overall performance of the tank, of 4.9 and 3.6, respectively.

### Component and System Tests

For operation with the 800 MeV booster synchrotron, the proton pulse from the linac had to be lengthened from 20 μsec to 100 μsec; during the last few years this has involved the modification of some of the major systems. In this context, the 3 MeV accelerator has been used for prolonged tests of the duoplasmatron source and the HV compensation at

100  $\mu$ sec beam pulse length.(7) The beam is subsequently chopped to  $< 30 \mu$ sec for acceleration through the cavity as the focusing system cannot handle long pulses. For a new RF level control system now under study the 3 MeV accelerator with its heavy beam loading will provide a realistic test substitute for the 50 MeV linac cavities.

#### Some Comments on the Engineering

The 3 MeV cavity mechanical design represents a considerable advance compared to the 50 MeV linac which was manufactured 10 years previously. Two of the factors which had most influence on the over-all design were the use of copper-clad steel (now universally preferred to the liner-in-a-vacuum-tank solution) and ultra-high vacuum techniques with metal seals throughout. On the cavity the main RF connections are made by the aluminium wire vacuum seals, for example on the end plates, the top girder, drift-tube stems, and the end half drift tubes; these joints have given no trouble. This copper-clad technology and the electron beam welded drift tubes with single support stem is certainly applicable to any future CERN linac. As mentioned before, the girder support and associated adjustment mechanisms have several clear advantages for mounting and alignment, but this approach might be difficult to apply to longer tanks of smaller diameter with larger ( $\sim 180$  mm diameter) drift tubes.

For the quadrupoles there are now good designs at other laboratories for  $N = 1$  operation from 750 keV injection. Our experience has shown that the quadrupoles can be run well into saturation and yet give a satisfactory quality beam. This way of running quadrupoles should not necessarily be rejected for the difficult region near 500 keV.

#### Conclusions

The aim of this paper is to give an over-all picture of the research and development associated with the 3 MeV experimental linac. In our experimental work at 500 keV many phenomena were observed, among which self-neutralization and the perturbing effects of secondary electrons were the most significant. Indications are that better transport and matching are required at 500 keV before one can fully exploit the possibilities of the present source and accelerating column. With the 3 MeV beam it has been shown that  $N = 1$  focusing starting at 500 keV is practicable and gives better transverse beam quality than the  $N = 2$  arrangement, especially above 100 mA. The ability to do extended beam measurements with RF fields and quadrupole gradients far beyond their normal working points is a distinct merit of an experimental accelerator. But an equally important function of the 3 MeV linac has been to provide a focal point for computational work on linacs, mechanical design and off-line component and system tests.

#### Acknowledgements

Many people have helped us on the 3 MeV accelerator during the past five years. Firstly, I would like to acknowledge the support and encouragement of C.S. Taylor who initiated the project. This

project has had few full-time staff so the conscientious work of A. Bellanger and H.F. Malthouse (also J.P. Buathier before 1970) is especially appreciated. Much interesting work was done in close collaboration with M. Martini and L. Evans, and for a short period with E. Dziura (from Swierk). E. Boltezar and the MPS Design Office were responsible for the successful mechanical design. For vital help, often at short notice, special thanks are due to F. Chiari and also to W. MacDonald, R. Dubois, F. Block and the many others concerned with source, mechanical maintenance, high-voltage and radio-frequency.

#### REFERENCES

- 1) E. Boltezar, H.F. Malthouse and D.J. Warner, A 3 MeV Experimental Proton Linac: Design, Construction and Proposed Experiments, Proc. 1968 Proton Linear Accelerator Conf., BNL, 1968, Part 2, p. 626.
- 2) L.R. Evans and D.J. Warner, Studies of Space-Charge Neutralization in Intense 500 keV Proton Beams, IEE Trans. Nuclear Sci. NS-18, 1068 (1971).
- 3) L.R. Evans and D.J. Warner, A Critical Study of Emittance Measurements of Intense Low-Energy Proton Beams, Nuclear Instrum. Methods, in press.
- 4) L.R. Evans and D.J. Warner, Real-Time Measurements of Proton Bunch Form, these Proceedings.
- 5) M. Martini and D.J. Warner, An Improved Method for Calculating Proton Linac Cavities, Proc. 1968 Proton Linear Accelerator Conf., BNL, 1968, Part 2, p. 512.
- 6) M. Martini and M. Promé, Beam Dynamics in a Proton Linac with Space Charge, Proc. VII Int. Conf. on High-Energy Accelerators, Yerevan, USSR, 1969, Vol. 1, p. 223.
- 7) R. Dubois, Compensating the Drop in Accelerating Voltage Caused by the Beam by Means of an Electronic Servo System, CERN/MPS/LIN 71-9 (1971):
- 8) E. Regenstreif, The CERN Proton Synchrotron (2nd Part), CERN 60-26 (1960).
- 9) B. Bru and M. Weiss, Linac Quadrupole Gradients and Matching Parameters at Different Beam Intensities, Proc. 1970 Proton Linear Accelerator Conf. NAL, 1970, Vol. 2, p. 851.

#### DISCUSSION

Bobylev, ITEP: What is the stability of radio-frequency field during the beam pulse?

Warner: There is no beam loading compensation, so as I mentioned, it varies by 1% per  $\mu$ sec for 200 mA. This is a short tank, so we don't expect any phase errors along the tank in our measurements, and we always measure our beam currents at one specific time in the pulse.

TABLE I

## CERN 3 MeV EXPERIMENTAL PROTON LINAC

ParametersPhysical Dimensions

Total length: 1.509 m. No. of tanks: 1.  
 Tank diameter: 1.076 m. No. of drift tubes:  $17 + 2 \times \frac{1}{2}$ .  
 Drift-tube lengths: 39.6 mm to 86.3 mm.  
 Drift-tube diameters: 140.3 mm to 120.9 mm.  
 Gap/Cell length: 0.25 (constant throughout).  
 Aperture diameter: 16.5 mm to 27.9 mm.

Ion Source

Type: Duoplasmatron.  
 Output: > 600 mA at 75 keV.

Injector

Type: high gradient, double gap.  
 Output: > 600 mA at 540 keV.  
 Beam emittance:  $\sim 150\pi$  mm mrad for 450 mA.

Buncher

Type: Single-gap, re-entrant.  
 Potential:  $\sim 17$  kV. Drift length: 0.82 m.

Acceleration System

TM<sub>010</sub> at 202.56 MHz, Q = 48,000.  
 Design equil. phase: 30°. Accel. rate: 1.68 MeV/m.  
 Pulse length: 250  $\mu$ sec at 1/sec.  
 Filling time: 150  $\mu$ sec.  
 Shunt impedance (Z): 36 M $\Omega$ /m.  
 $Z = \{[\int_0^L |E(z)| dz]^2 / \text{Total power dissipated}\} \times 1/L$ .  
 RF power input: 280 kW peak, 70 W mean.

Focusing System

18 pulsed quadrupoles, ++-- ( $\equiv N=2$ ) [or +-+- ( $\equiv N=1$ )].  
 Gradients: 7.3 (10.2) kG/cm to 2.0 (4.2) kG/cm.

Performance

Output energy: 3.05 MeV.  
 Energy spread: 2.5% FWHM.  
 Maximum currents: 140 mA (++--),  
 230 mA (+--+).  
 Beam emittances: 113 mA in  
 $5\pi \times 10^{-6}$  rad m (normalized by  $\beta\gamma$ ) ++--,  
 160 mA in  
 $7.5\pi \times 10^{-6}$  rad m (normalized by  $\beta\gamma$ ) +-+-.

NB. More details of operating levels and performance are given in the text.

TABLE II

## TYPICAL OPTIMUM CURRENTS FOR N = 1 AND N = 2

	N = 1	N = 2
Source current (mA)	$\sim 700$	$\sim 700$
Cavity input current (mA)	420	420
Total output current (mA)	275	165
Analysed 3 MeV current (mA)	225	145
Transmission factor	0.54	0.35
Bunching factor	1.9	1.8
Corresponding $\phi_s$	$\sim 39^\circ$	$\sim 29^\circ$
Quadrupole field law	$\beta' \propto \beta^{-1}$	$\beta' \propto \beta^{-1.5}$
Maximum gradient	102 T m <sup>-1</sup>	73 T m <sup>-1</sup>

TABLE III

## EMITTANCE MEASUREMENTS IN z, z' PLANE

Result number	N	Current (mA)	Emittances <sup>b)</sup>		
			$\epsilon_0$	$\epsilon_{rms}$	$\epsilon_{100}$
1	1	180	3.3	7.4	2.5
2	1	168	2.2	5.4	1.9
3 <sup>a)</sup>	1	97	2.2	5.3	-
4	2	121	2.2	5.0	4.4
5	2	128	2.1	5.0	3.5

a) Result 3 obtained without buncher.

b) Emittances are area  $\times \beta\gamma/\pi$  in mm mrad.

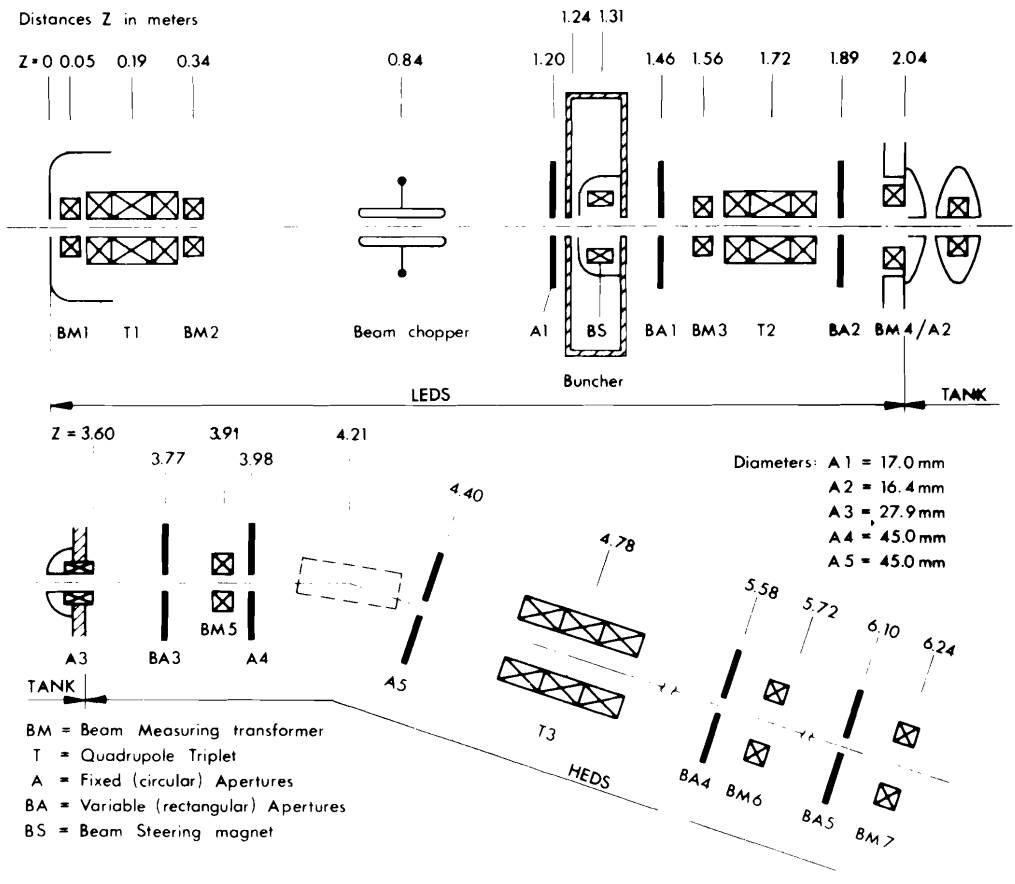


Fig. 1 Schematic Layout of 3 MeV Accelerator

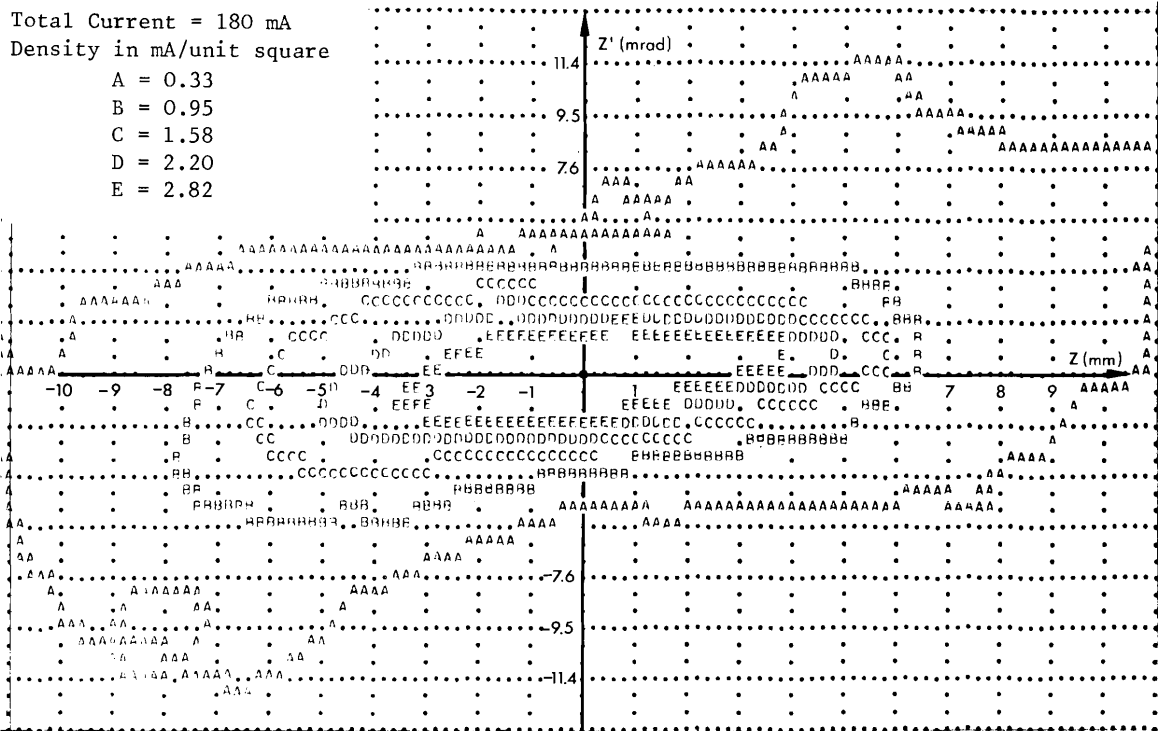


Fig. 3 Emittance in z, z' as analyzed by EMITNC

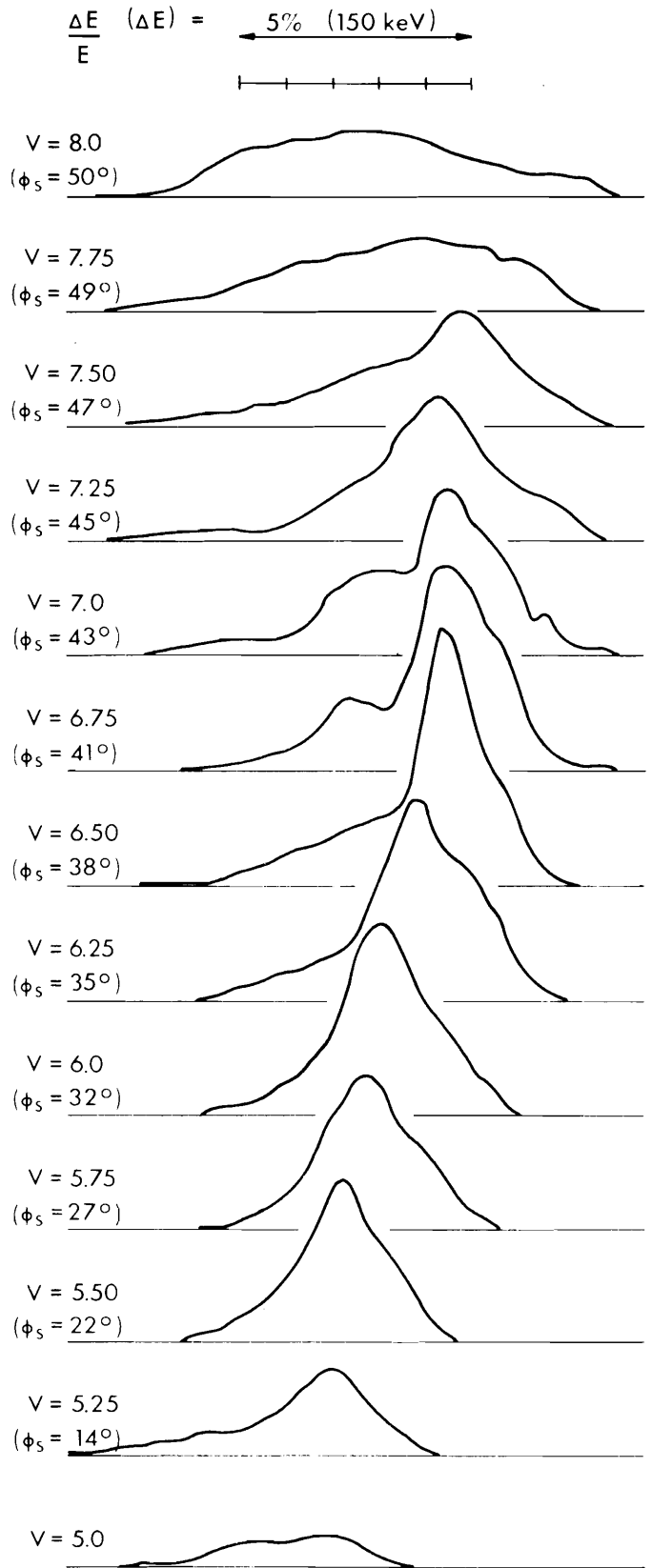
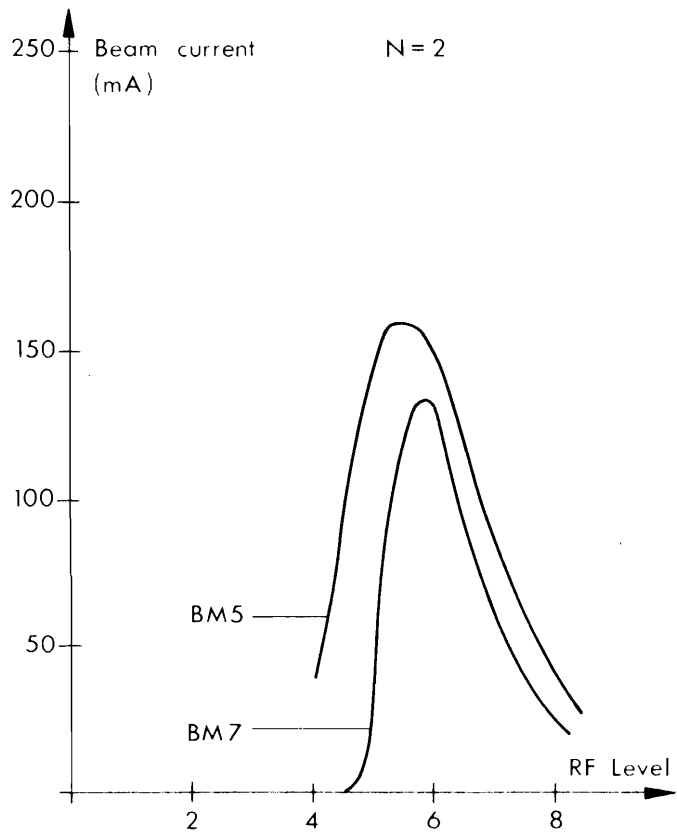
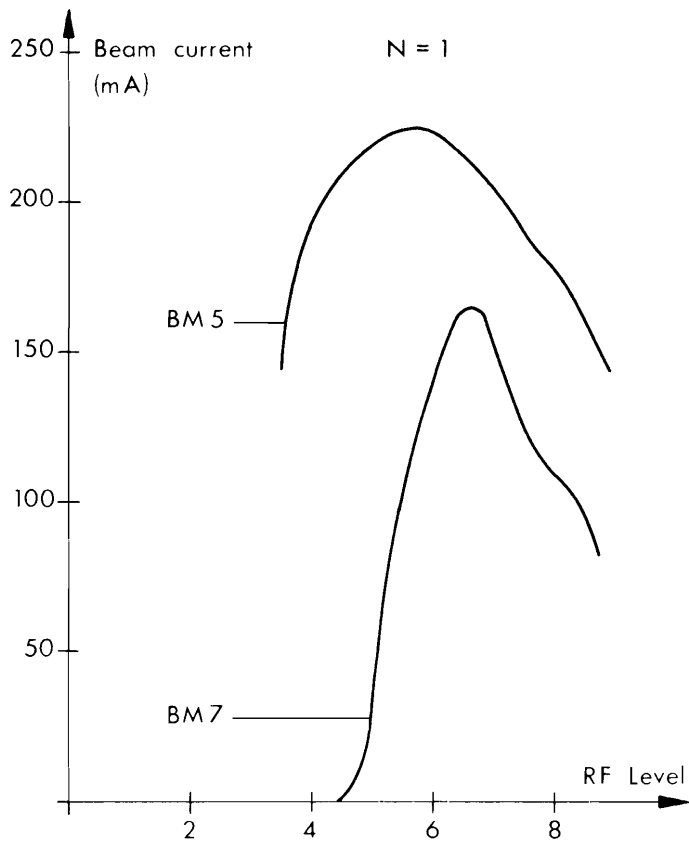


Fig. 2 Current Out of Linac as function of RF Levels

Fig. 4 Energy Spectra as function of RF Levels